Investigation of the Transmitter Susceptibility to Reverse Intermodulation by the Use of Double-Frequency Diagrams

Eugene Sinkevich, Vladimir Mordachev
EMC R&D Laboratory
Belarusian State University of Informatics and Radioelectronics
Minsk, Belarus
emc@bsuir.by

Abstract—A technique for detection of reverse intermodulation components (which are generated if an external interfering signal received by the transmitting antenna influences on the output stages of the transmitter) by measuring the interference frequency response of the transmitter output spectrum and visualizing that response as a double-frequency diagram is developed. A technique for automated recognition (identification) of the reverse intermodulation types and orders on the basis of the double-frequency diagram is proposed. Both techniques are validated by the experiments. Amplitude responses for reverse intermodulation components of various types and orders are measured.

Keywords—immunity testing; measurement techniques; radio transmitters; microwave amplifiers; radiofrequency interference

I. Introduction

Reverse intermodulation (which is also referred to as back intermodulation) is generated in a transmitter if one or several antenna-induced interfering signals influence on the transmitter output [1, pp. 791-798], [2, pp. 37, 56], [3]. For co-located transmitters and for transmitters sharing a common antenna via multiplexer circuits, the reverse intermodulation is especially dangerous because it may predominate (by the level) over the receiver intermodulation and over the passive intermodulation generated in components of neighboring structures (radio mast, ship hull, etc.) – the examples of such domination are given in [4], [5], [6], [7]. Therefore, it is important to account for the reverse intermodulation in transmitters when analyzing electromagnetic compatibility (EMC) of radio and microwave equipment.

The objective of this paper is to develop a technique for experimental analysis of the reverse intermodulation components, including their detection, their recognition (i.e., determination of their types and orders), and measurement of their characteristics and parameters.

For reliable detection and recognition of the reverse intermodulation components (and of the other nonlinear effects caused by the impact of the powerful interfering signals on the transmitter output – frequency capture and pulling, spurious generation, nonlinear noise [8], [9]), a technique of panoramic

measurement of the transmitter EMC characteristics by the instrumentality of a double-frequency test system was developed and used successfully [8]. The technique is based on the automated sweep of the test signals' frequencies (each test signal simulates an interfering signal).

In this paper, an improved panoramic technique which makes it possible to simplify the measurement setup and to reduce the measurement time is developed (Section II). Then a procedure for automated recognition of the reverse intermodulation components detected by the use of the improved panoramic technique is proposed (Section III). After that, the measured amplitude characteristics of the reverse intermodulation components are discussed (Section IV), and the peculiarities of the reverse intermodulation measurement are considered (Section V).

II. Detection of Nonlinear Effects in Transmitter the Output of which Is Influenced by Interfering Signal

A. Double-Frequency Testing of Transmitters

A measurement setup for detection of nonlinear effects in a transmitter by the double-frequency test technique (DFTT) is shown in Fig. 1 [8]. A two-tone signal (which simulates two interfering signals) synthesized by the instrumentality of two measuring generators is fed to the output of the transmitter under test. The transmitter output signal, which includes the reverse intermodulation among other components, is measured by the spectrum analyzer tuned to the fixed frequency f_r (i.e., working in "Zero span" mode). The spectrum analyzer simulates a receiver operating in one of the adjacent (to the transmitter under test) frequency channels. Ferrite circulator provides the decoupling, i.e., it suppresses both the transmitter-under-test signal appearing at the outputs of the measuring generators and the measuring generators' signals appearing at the input of the spectrum analyzer.

The powers (P_1, P_2) of the measuring generators' output signals are constant, and their frequencies are sweeping synchronously by the saw-tooth law (similarly to the signals of horizontal and vertical sweeps of a kinescope) [10]. This makes

it possible to measure the dependence of the level P_{out} of transmitter output spectrum components falling within the relatively narrow band Δf_r of the spectrum analyzer on the frequencies (f_1, f_2) of the measuring generators' signals:

$$P_{out}(f_1, f_2), \qquad (P_1, P_2, f_r, \Delta f_r) = const . \qquad (1)$$

This dependence is referred to as the double-frequency characteristic (DFC) and it is usually visualized as a color map called the double-frequency diagram (DFD) [8].

In practice, it is often necessary to characterize the transmitter-generated nonlinear products falling within each of dozens of the adjacent channels. In this case, a set of DFCs (1) must be measured at different tuning frequencies f_r of the spectrum analyzer [8].

The powers P_1, P_2 of the test signals are determined on the basis of a forecast of the electromagnetic environment in the place of the transmitter antenna. If there is no such forecast, the powers are taken from the standards (their values are usually 15…60 dB less than the power P_t of the desired signal at the transmitter output) [11, CE111], [12], [13], [14], [15].

B. Single-Frequency Testing of Transmitters

The experience of DFTT application to measurement of the reverse intermodulation shows that it is possible to simplify the test setup and to decrease the measurement time without notable loss of the retrieved information about the nonlinear properties of the transmitter. For that purpose, it is necessary to exclude one measuring generator from the test setup (Fig. 2) and to sweep the tuning frequency of the spectrum analyzer, i.e., to measure the dependence of the transmitter output spectrum on the interfering signal frequency:

$$P_{out}(f_1, f_r), \qquad (P_1, \Delta f_r) = const . \qquad (2)$$

This dependence is called the double-frequency spectrogram (DFS). Similarly to the time-frequency spectrogram (which is widely used, e.g., in digital speech processing [16]), the DFS may be interpreted as a one-dimensional Fourier transform of the bivariate function over one of the arguments of that function.

Like the DFC, the DFS can be visualized as a three-dimensional plot (Fig. 3) or as a color map (DFD, Fig. 4). Vertical lines in the DFD represent the transmitter output spectrum components that are independent on the interfering signal frequency (such as the fundamental emission at the frequency $f_t = 2.00$ GHz and the spurious emissions at the frequencies $f_{s1} = 1.97$ GHz, $f_{s2} = 2.03$ GHz shown in Fig. 4). The straight line $f_1 = f_r$ located on the DFD diagonal 45º corresponds to the measuring generator signal; the other inclined lines are the images of reverse intermodulation components (ref. Section III). Curvilinear images (lines and areas) in the DFD represent specific nonlinear effects:

frequency capture and pulling, spurious generation and (or) nonlinear noise appearing in a certain band of the interfering signal frequencies, intermodulation caused by mixing of the test signal with the above-mentioned spurious generation [8], [9]. Similar specific effects were found in receivers [17].
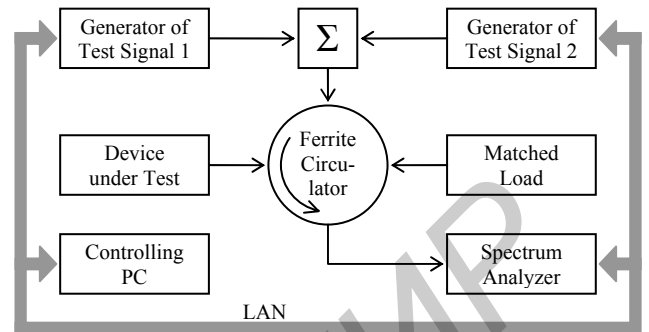

Fig. 1. Test setup for conducted measurement of the reverse intermodulation in a transmitter by the double-frequency test technique (DFTT)
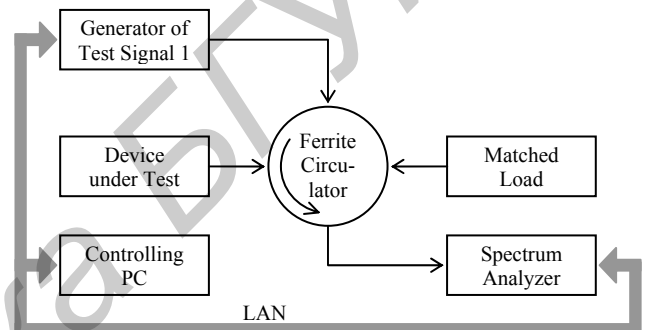

Fig. 2. Test setup for conducted measurement of the reverse intermodulation in a transmitter by the single-frequency test technique (SFTT)
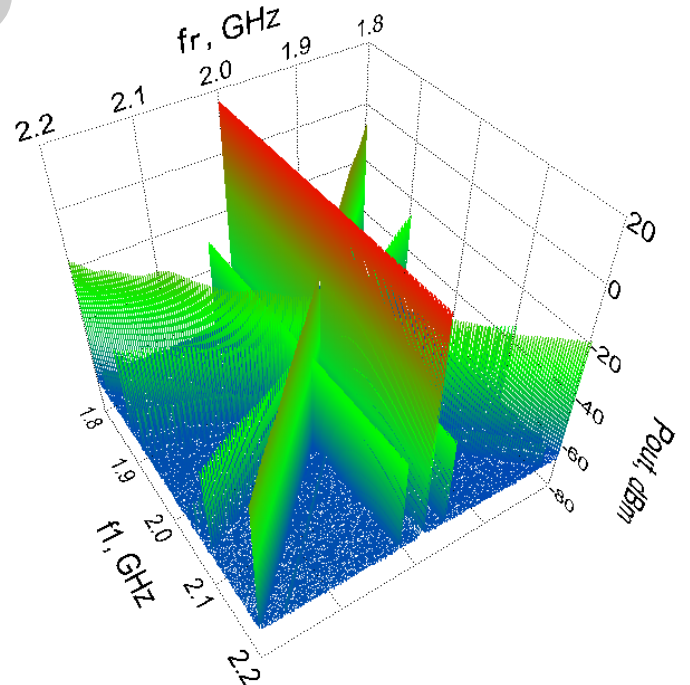

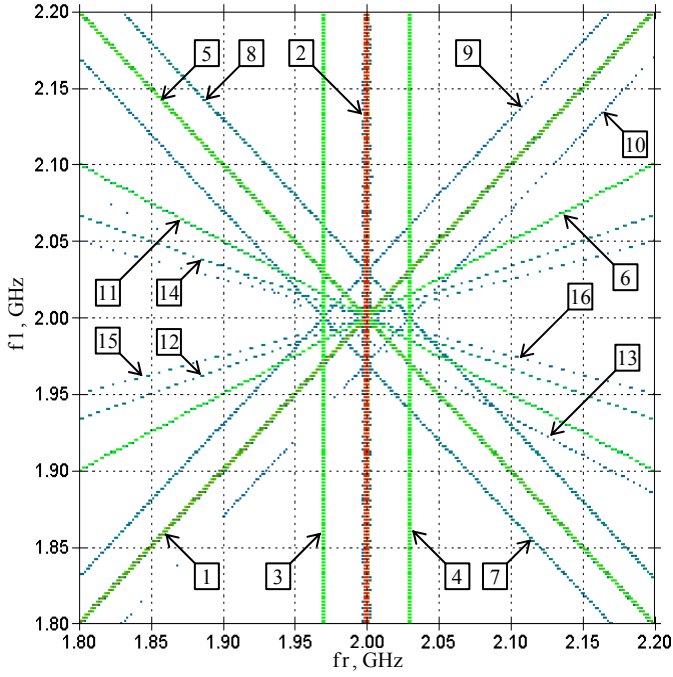Fig. 3. Three-dimensional plot of the double-frequency spectrogram (DFS)

Fig. 4. Double-frequency diagram (DFD), which is a color map of the double-frequency spectrogram (DFS) shown in Fig. 3. The display threshold is of -62 dBm

The proposed technique of single-frequency testing (SFTT, ref. Fig. 2) may be interpreted not only as a special case of the DFTT [8] (ref. Fig. 1) but also as a generalization of the standard techniques for measurement of reverse intermodulation levels in transmitters and oscillators [11, CE111], [12], [13], [14], [15]. In contrast with the standard techniques, the SFTT requires to change the frequency of the test signal (which simulates the interfering signal). This makes it possible to reliably recognize the types and orders of the reverse intermodulation components generated in the device under test (ref. Section III).

III. RECOGNITION OF REVERSE INTERMODULATION TYPES AND ORDERS

A. Recognition Technique

Generation of the reverse intermodulation components in a transmitter and their measurement by the instrumentality of a spectrum analyzer can be described by the following equation, which is referred to as a channeling equation:

$$f_{IM} = z_1 f_1 + z_2 f_2 + z_3 f_t + z_4 f_{s1} + z_5 f_{s2} = f_r, \quad (3)$$

where f_{IM} is the frequency of the reverse intermodulation component; $z_1...z_5$ are integer coefficients; f_1 and f_2 stand for the frequencies of the first and second test signals fed to the transmitter output (ref. Fig. 1); f_t is the fundamental emission frequency of the transmitter under test; f_{s1}, f_{s2} are the frequencies of the transmitter's spurious emissions; f_r is the tuning frequency of the spectrum analyzer.

Equation (3) generalizes the reverse intermodulation generation equations given in standards [11, CE111], [14], [15].

If the transmitter is tested by the DFTT (ref. Fig. 1), equation (3) should be written as

$$z_1 f_1 + z_2 f_2 + C = 0, \quad C = f_{NL,t} - f_{out}, \quad f_{out} = f_r, \quad (4)$$

where $f_{NL,t}$ denotes the frequency of a (existing or imaginary) combination component generated by the fundamental and spurious emissions of the transmitter:

$$f_{NL,t} = \begin{cases} z_3 \cdot f_t, & N_{fs} = 0; \\ z_3 \cdot f_t + z_4 \cdot f_{s1}, & N_{fs} = 1; \\ z_3 \cdot f_t + z_4 \cdot f_{s1} + z_5 \cdot f_{s2}, & N_{fs} = 2, \end{cases} \quad (5)$$

N_{fs} is the number of spurious emission components in the output spectrum of the transmitter under test.

In compliance with (4), each reverse intermodulation component is displayed as a straight line on the double-frequency diagram in coordinates (f_1, f_2). The problem of reverse intermodulation identification (recognition) is to find values of the coefficients $z_1...z_5$ in channeling equation (3), based on the given image of the intermodulation component in the double-frequency diagram. Having these values, one can determine the transmitter output spectrum components generating the recognized intermodulation product and find the slope (dB/dB) of the amplitude characteristic for that product (ref. Section IV).

Since (4) coincides with the channeling equation for a receiver (only the physical meaning of some variables is changed), the recognition of responses detected in the DFC (1) of a transmitter can be performed by the technique developed in [10]. According to (3), the order M of a reverse intermodulation component is calculated as

$$M = \sum_{k=1}^{5} |z_k|. \quad (6)$$

If the transmitter is tested by the SFTT (ref. Fig. 2), the test signal having the frequency f_2 is absent, and equation (3) takes the form

$$f_{IM} = z_1 f_1 + z_3 f_t + z_4 f_{s1} + z_5 f_{s2} = f_r. \quad (7)$$

Let us represent (7) in a form which is similar to (4):

$$z_1 f_1 + z_2 f_r + C = 0, \quad f_{out} = 0, \quad z_2 = -1, \quad (8)$$

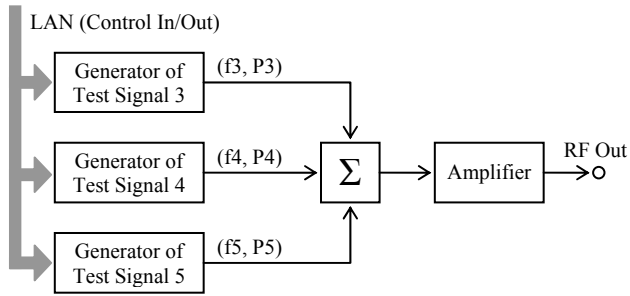where C and $f_{NL,t}$ are defined by (4) and (5).

Fig. 5. Transmitter-under-test model intended for validation of the reverse intermodulation recognition technique
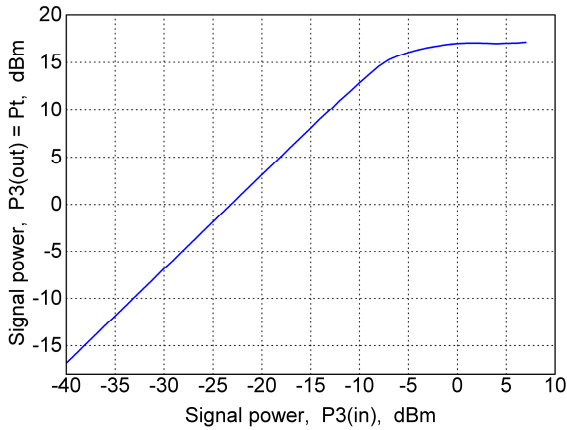

Fig. 6. Single-tone amplitude characteristic of amplifier "Mini-Circuits ZKL-2R7+" (ref. Fig. 5), which is measured at the frequency of 2 GHz

TABLE I. COMPONENTS DETECTED IN DOUBLE-FREQUENCY DIAGRAM (DFD, FIG. 4) OF THE TRANSMITTER MODEL (FIG. 5)

Type of component	No	Order of intermodulation	Coefficients in (7)			
			$z1$	$z3$	$z4$	$z5$
Test-signal	1	{1}	1	0	0	0
Fundamental	2	{1}	0	1	0	0
Spurious	3	{1}	0	0	1	0
	4	{1}	0	0	0	1
Intermodulation	5	3 (H)	-1	2	0	0
	6	3 (L)	2	-1	0	0
	7	3	-1	1	1	0
	8	3	-1	1	0	1
	9	3	1	1	0	-1
	10	3	1	-1	0	1
	11	5 (H)	-2	3	0	0
	12	5 (L)	3	-2	0	0
	13	5	-2	2	1	0
	14	7 (H)	-3	4	0	0
	15	7 (L)	4	-3	0	0
	16	9 (H)	-4	5	0	0

In compliance with (8), each reverse intermodulation component is displayed as a straight line on the double-frequency diagram in coordinates (f_1, f_r). That is why the technique [10] can be used for recognition of responses detected in the DFS (2) of a transmitter – for that purpose, it is necessary to modify the technique as follows (compare (8) with

(4)): 1) to take $f_2 = f_r$, $f_{out} = 0$, $z_2 = -1$, i.e., to jump the exhaustive search over the variable z_2; 2) based on (7), to calculate the order M of a component as

$$M = |z_1| + \sum_{k=3}^{5} |z_k|. \qquad (9)$$

B. Validation of the Recognition Technique

For validation of the proposed recognition technique, a SFTT setup was composed (ref. Fig. 2). Output stages of the transmitter under test are simulated by amplifier "Mini-Circuits ZKL-2R7+" (Fig. 5), which has the following parameters: the working frequency band is 10…2700 MHz, the output power at 1-dB-compression point is 15.4 dBm, and the gain is of 23.1 dB (Fig. 6). The sum of signals from several measuring generators is fed to the amplifier input: generator 3 simulates the fundamental emission of the transmitter, and the other generators are intended for imitation of spurious emissions in the transmitter output spectrum.

As an example, let us consider the DFS measurement results given in Figs. 3 and 4. Those results are obtained under the following conditions. The range of frequency sweep for both generator 1 and spectrum analyzer is as follows: $f_1, f_r \in [1.8; 2.2]$ GHz; the sweep resolution is 201 points by frequency f_1 (i.e., the step $\Delta f_1 = 2$ MHz) and 1001 points by frequency f_r (the step $\Delta f_r = 400$ kHz); the resolution bandwidth of the spectrum analyzer $RBW = 820$ kHz. Generators 3 and 4 operate at fixed frequencies $f_3 \equiv f_t = 2000$ MHz, $f_4 = 2030$ MHz, generator 5 is not in use. The test signals are not modulated, and they have the following levels (referred to the amplifier ports): $P_{1(out)} = 5$ dBm, $P_{3(in)} = 0$ dBm, $P_{4(in)} / P_{3(in)} = -40$ dB. The amplifier operates in saturation mode ($P_{3(out)} \equiv P_t = 17$ dBm), therefore, the components with frequencies $f_{s1} = 2f_t - f_4 = 1970$ MHz, $f_{s2} = f_4 = 2030$ MHz are observed in its output spectrum. The DFS measurement takes 30 seconds if the video bandwidth of $VBW = 82$ kHz and 10 trace averages are used in the spectrum analyzer.

All components detected in the DFD (Fig. 4) have been correctly recognized by the proposed technique in automated mode (based on the marker line method [18], [10]). The recognition results are given in Table I.

Similar results are obtained for the DFSs measured in 0-th, 2-nd, and 3-rd-order harmonic zones.

IV. MEASUREMENT OF REVERSE INTERMODULATION CHARACTERISTICS AND PARAMETERS

After the recognition of the reverse intermodulation components, it is often necessary to perform their detailed analysis, i.e., measurement of their levels (or some other characteristics of their interfering impact on the receptor) depending on the amplitude and (or) frequency of the interfering and (or) desired signal at the device-under-test

output. The detailed experimental analysis of classical 3-rd-order intermodulation is well described in literature [19], [20], [21, pp.19-21], [22], [23, p.58], [6, pp.34-42], but the reported experimental results devoted to the reverse intermodulation of other types and orders are limited by measured coefficients of the linearized behavioral model [24], [4].

The amplitude characteristics of the reverse intermodulation components of various types and orders are given in Fig. 7. These characteristics are measured at 1-dB-compression point $P_{3(out)} \equiv P_t = 15.4$ dBm of amplifier "Mini-Circuits ZKL-2R7+" (ref. Figs. 5 and 6). Similar measurements are performed for the other values of the desired signal power, both in linear mode ($P_t \in \{8.1, 12.9\}$ dBm, Fig. 8) and in saturation mode ($P_t = 17$ dBm) of the amplifier.

The interfering signal frequency f_1 should be set in such a manner that the frequencies (7) of intermodulation components of different types and orders do not coincide. It is convenient to use the DFD for this purpose (ref. Fig. 4): the lines in the DFD should not cross at the selected value of f_1.

The results of measurements show the applicability of the linearized behavioral model [24] to the reverse intermodulation (of orders 3, 5, and 7) generated in amplifier "Mini-Circuits ZKL-2R7+" if the signal-to-interference ratio $P_t / P_{1(out)} \equiv C/I \geq 15$ dB (ref. Figs. 7 and 8). That model represents each amplitude characteristic as a straight line the slope (dB/dB) of which is equal to the absolute value of coefficient z_1 (ref. Table I and Figs. 7, 8).

V. PECULIARITIES OF REVERSE INTERMODULATION MEASUREMENTS

A. Checking the Validity of Measurements

The following techniques were used for checking the validity of measurements performed in this work.

At the beginning of measurements it is important to prove that observed intermodulation components (and the other nonlinear effects) are generated in the device under test, and not in the measurement setup. For this purpose, the device under test should be replaced by a higher-quality source of signal (e.g., by a source that contains the protection elements or has a higher maximal power) in such a manner that the desired signal level remains unchanged. As a result of the replacement, the measured power of intermodulation products must decrease at least by 10 dB (which corresponds to systematic measurement error of 0.4 dB), otherwise we should not neglect the intermodulation generated in the measurement setup.

In order to find the source of intermodulation generated in the measurement setup, the standard technique can be used [11, CS110], [14], [15]: connect a 3 dB attenuator to the spectrum analyzer input and check the result – if the measured level of the intermodulation product decreases by more than 3 dB then the spectrum analyzer is a source of the intermodulation, otherwise the intermodulation is generated by the measuring generators or by the other components of the measurement setup (circulators, directional couplers, connectors, etc.)
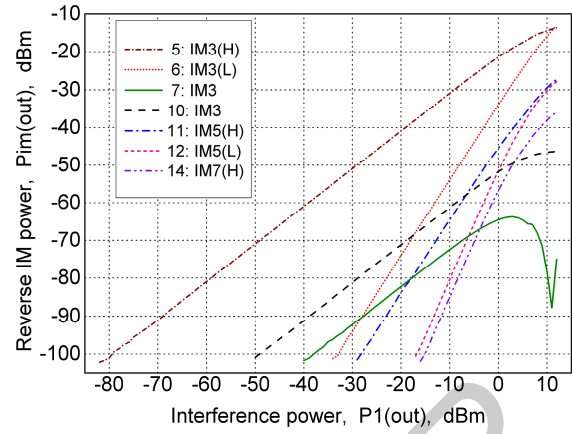

Fig. 7. Amplitude characteristics of reverse intermodulation components (ref. Table I) generated in amplifier "Mini-Circuits ZKL-2R7+" (ref. Figs. 5 and 6). Parameters of measurements (ref. Fig. 2): desired signal power $P_t = 15.4$ dBm, its frequency $f_t = 2000$ MHz, interfering signal frequency $f_1 = 2051$ MHz, bandwidth of the spectrum analyzer $\Delta f_r = 200$ Hz, measurement step $\Delta P_{1(out)} = 1$ dB
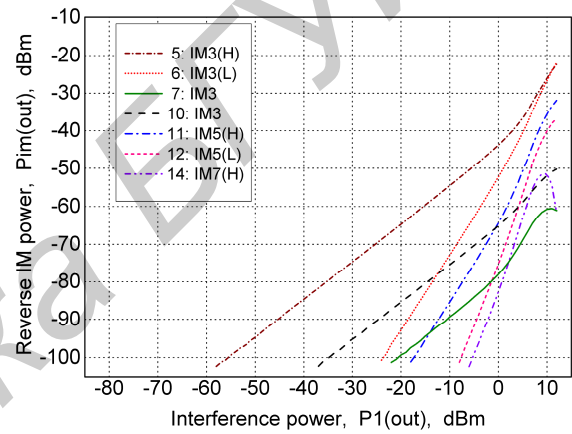

Fig. 8. Amplitude characteristics of reverse intermodulation components generated in amplifier "Mini-Circuits ZKL-2R7+". Parameters of measurements are the same as in Fig. 7, but $P_t = 12.9$ dBm

During the measurements of the amplitude (or frequency) responses of intermodulation components (ref. Section IV), it is important to check the type of the measured product: an intermodulation component disappears if the source of any signal taking part in generation of the component is switched off [11, CE111], [14], [15].

B. Possible Improvements in the Measurement Setup

The measurement setup shown in Fig. 2 makes it possible to demonstrate the meaning and structure of the DFS in the best way (ref. Figs. 3 and 4). But it has the following drawbacks which limit the dynamic range of the measurements (i.e., they limit the minimal measurable level of intermodulation products): 1) a powerful output signal of the device under test is fed to the spectrum analyzer input; 2) that signal (attenuated by 15…25 dB, which is typically provided by a circulator) impacts also on the measuring generator output – this may cause the origination of reverse intermodulation in the measuring generator; 3) the measuring generator output signal attenuated by the same 15…25 dB

influences on the spectrum analyzer input; 4) intermodulation may be caused by nonlinearity of the circulator.

To eliminate the mentioned drawbacks, the filtering and (or) cancellation of undesired signals, as well as the directional couplers are usually applied [11, CE111], [14], [15], [12], [13], [25], [26], [19], [27, p. 2227], [28]. It is also possible to adapt the automated cancellation techniques developed for measurements of passive intermodulation levels [29]. In order to reduce the influence of mismatch errors, it is recommended to couple a 10 dB attenuator to the transmitter-under-test output with the shortest possible connection [12], [13].

If it is impossible or unreasonable to disconnect the antenna from the transmitter under test (e.g., as a result of a high sensitivity of reverse intermodulation levels to the change of transmitter output matching – this change may be caused by the replacement of the antenna by the dummy load), the measurements should be performed by field (i.e., as a radiated measurements) [14], [7, Fig. 11].

VI. CONCLUSION

The results of the reverse intermodulation measurements may be used for analysis and diagnostics of intrasystem and intersystem EMC.

The developed techniques can be applied to analysis of reverse intermodulation generated not only in transmitters but also in RF/microwave components (oscillators, amplifiers) that may be used as output stages of transmitters [15], [19], [20].

High efficiency of the developed techniques for detection and recognition of reverse intermodulation (ref. Sections II and III) is confirmed by practice. Based on the techniques, the corresponding functionality in the double-frequency test system of the new generation is implemented [30].

REFERENCES

[1] R. Perez (ed.), Handbook of Electromagnetic Compatibility. San Diego, CA: Academic Press, 1995.

[2] W.G. Duff, Designing electronic systems for EMC. Raleigh, NC: SciTech, 2011.

[3] A.L. Badalov, A.S. Mikhailov, Limits on EMC parameters of radio equipment. Handbook. Moscow: Radio i Sviaz, 1990 (in Russian).

[4] J. Gavan, "Main effect of mutual interference in radio communication systems using broad-band transmitters," IEEE Trans. EMC, vol. 28, no. 4, pp. 211-219, 1986.

[5] K. Allsebrook, C. Ribble, "VHF cosite interference challenges and solutions for the United States Marine Corps' expeditionary fighting vehicle program," IEEE Military Comm. Conf. MILCOM 2004, vol. 1, pp. 548-554.

[6] Comments of Qualcomm Incorporated, WT Docket No. 12-69 (filed June 1, 2012), http://apps.fcc.gov/ecfs/document/view?id=7021921420

[7] S. Ahmed, M. Faulkner, "Mitigation of reverse intermodulation products at colocated base stations," IEEE Trans. Circuits and Systems I: Regular Papers, vol. 60, no. 6, pp. 1608-1620, 2013.

[8] V.I. Mordachev, "Automated double-frequency testing technique for mapping receive interference responses," IEEE Trans. EMC, vol. 42, no. 2, pp. 213-225, 2000.

[9] V.I. Mordachev, "Computer-aided double frequency testing system," Int. Conf. "New information technologies for science and industry", Minsk, Belarus, Nov. 24-27, 1998, pp. 223-228.

[10] V.I. Mordachev, E.V. Sinkevich, "Experimental analysis of radio receiver susceptibility to out-of-band interference by means of double-frequency test system," 10-th Int. Symp. on EMC "EMC Europe 2011", UK, York, Sept. 26-30, 2011, pp. 405-411.

[11] Standard, Military. Radio Frequency Spectrum Characteristics Measurement of. (MIL-STD-449D). USA Department of Defense, Washington, 1973.

[12] Recommendation ITU-R SM.1446-0 (2000), Definition and measurement of intermodulation products in transmitter using frequency, phase, or complex modulation techniques.

[13] ETSI EN 300 086-1 V1.4.1 (2010-06). European Standard (Telecommunications series) "Electromagnetic compatibility and Radio spectrum Matters (ERM); Land Mobile Service; Radio equipment with an internal or external RF connector intended primarily for analogue speech; Part 1: Technical characteristics and methods of measurement."

[14] GOST R 50842-95. Russia State Standard "Electromagnetic compatibility of radioelectronic equipment. Radio transmitting devices for national economic application. Limits for spurious emissions. Measuring and monitoring methods". Moscow, 1996 (in Russian).

[15] GOST R 50638-94. Russia State Standard "EMC of technical equipment. Semiconductor microwave oscillator devices and modules. List of EMC parameters and requirements for them. Methods of measurement". Moscow, 2004 (in Russian).

[16] L.R. Rabiner, R.W. Schafer, "Introduction to digital speech processing", Foundations and trends in signal proc., vol. 1, no. 1, pp. 1-194, 2007.

[17] V. Mordachev, E. Sinkevich, D. Petrachkov, "Representation and analysis of radio receivers' susceptibility and nonlinearity by the use of 3D double-frequency characteristics," 2014 Int. Symp. on EMC (EMC'14/Tokyo), IEEE, 2014, pp. 689-692.

[18] E. Sinkevich, "Universal technique for interference response recognition from results of radio receiver's double-frequency testing," IX-th Int. Symp. on EMC and Electromagnetic Ecology, Saint-Petersburg, Russia, Sept 13-16, 2011, pp. 308-311.

[19] A. Katz, D. McGee, C. Brinton, and J. Qiu, "Sensitivity and mitigation of reverse IMD in power amplifiers," IEEE Topical Conf. on Power Amplifiers for Wireless and Radio Appl. (PAWR), 2011, pp. 53-56.

[20] M. Kamper, G. Ulbricht, R. Weigel, G. Fischer, "Comparison of class A and class D RF amplifier operation with focus on reverse intermodulation and efficiency performance," 2011 European Microwave Integrated Circuits Conf. (EuMIC), pp. 272-275.

[21] S. Ahmed, Interference mitigation in colocated wireless systems. PhD dissertation, Victoria University, Melbourne, Australia, 2012.

[22] J.G. Holey, E.W. Wood, "A comparison of the spectrum signatures of AM, FM, and SSB communications equipments," 7th Conf. on RFI and EMC, Nov. 1961, pp. 140-172.

[23] D.R. Lohrmann, W.D. Patterson, Replacement of RT-524/246 transmitter tubes by transistor inserts. Techn. Rep. ECOM-4419, 1976.

[24] M.A. Maiuzzo, E. Mackouse, "Transmitter intermodulation product amplitudes," Int. Symp. on EMC, IEEE, 1981, pp. 133-138.

[25] J. Gavan, "Analysis of intermodulation between broadband frequency transmitters on mobile radio networks," Int. Symp. on EMC, IEEE, 1982, pp. 23-30.

[26] W.-C. Chang, "How to perform intermodulation distortion measurements for ferrite circulators and isolators," 2007, http://www.eetimes.com/document.asp?doc_id=1276252&print=yes

[27] K. Chang (ed.), Wiley encyclopedia of RF and microwave engineering, 6 Volume Set. Hoboken, NJ: Wiley, 2005.

[28] X. Li, "Analysis on reverse intermodulation generated by co-siting multi standard base stations," Applied Mechanics and Materials, vol. 433, pp. 1545-1548, 2014.

[29] J.M. Wetherington, M.B. Steer, "Robust analog canceller for high-dynamic-range radio frequency measurement," IEEE Trans. MTT, vol. 60. no. 6, pp. 1709-1719, 2012.

[30] Automated double-frequency test system. Documentation set (vol. 1 "User's manual", vol. 2 "Technical report"). Minsk, 2015.